



# EDGEWOOD

## CHEMICAL BIOLOGICAL CENTER

U.S. ARMY RESEARCH, DEVELOPMENT AND ENGINEERING COMMAND

**ECBC-CR-067**  
**(MRC-R-1597)**

### NEXT GENERATION LWIR SPECTRUM PROJECTOR (CB-2) DESIGN STUDY

**M.C. Thomas**



**Mission Research Corporation**  
**Santa Barbara, CA 93102**

**June 2004**

Approved for public release;  
distribution is unlimited.

**20040721 077**

**ABERDEEN PROVING GROUND, MD 21010-5424**

#### **Disclaimer**

**The findings in this report are not to be construed as an official Department of the Army position unless so designated by other authorizing documents.**



**Blank**

## **PREFACE**

**The work described in this report was authorized under Contract No. DAAD05-99-P-1008. This work was started in March 1999 and completed in September 1999.**

**The use of either trade or manufacturers' names in this report does not constitute an official endorsement of any commercial products. This report may not be cited for purposes of advertisement.**

**This report has been approved for public release. Registered users should request additional copies from the Defense Technical Information Center; unregistered users should direct such requests to the National Technical Information Service.**

**Blank**

## CONTENTS

1.	Introduction.....	1
2.	CB-2 Requirements.....	1
3.	CB-2 Design Overview.....	1
4.	CB-2 Design Trade-Offs.....	3
4.1.	Refractive Spectramitter, CB-2A.....	3
4.1.1.	Fiber Exit Slit.....	4
4.1.2.	CB-2A Optical Layout and Performance Estimates.....	6
4.1.2.1.	CB-2A Short Wave Analysis.....	6
4.1.2.2.	CB-2A Long Wave Analysis.....	8
4.1.3.	CB-2A Output Collimator.....	10
4.1.4.	CB-2A Conceptual Layout Diagrams.....	10
4.1.5.	CB-2A Spectral Resolution.....	11
4.1.6.	CB-2A Radiance Estimates.....	11
4.1.7.	CB-2A Performance Estimates.....	11
4.2.	CB-2A Reflective Spectramitter.....	13
4.2.1.	CB-2B Output Fiber Array and Mixing Rod.....	15
4.2.2.	CB-2B Output Collimator.....	16
4.2.3.	CB-2B System Performance.....	17
5.	System Comparisons and Discussion.....	18
	Reference.....	18

## FIGURES

1.	Fiber area variation with radius relative to ordinary slit.....	5
2.	Silver Halide attenuation plot .....	6
3.	CB-2A short wave ray trace diagrams .....	6
4.	CB-2A short wave ray traces .....	7
5.	CB-2A short wave spot diagrams for three wavelengths.....	7
6.	CB-2A short wave encircled energy and PSF plots for 9 $\mu\text{m}$ .....	7
7.	CB-2A long wave ray trace diagrams .....	8
8.	CB-2A long wave ray trace diagrams .....	9
9.	Spot diagrams for long-wave CB-2A .....	9
10.	CB-2A Spot diagrams and encircled energy diagrams for 11.6 $\mu\text{m}$ .....	9
11.	CB-2A collimator ray trace diagram and spot diagrams .....	10
12.	Top and perspective views of conceptual layouts of the CB-2A system.....	10
13.	Fiber area profile and typical emitted PSF for CB-2A and CB-2A predicted spectral resolution.....	11
14.	Ray trace diagram and spot diagram for short wave CB-2B .....	14
15.	Ray trace and spot diagrams for long-wave CB-2B .....	14
16.	Encircled energy diagram and PSF cross section for short wave CB-2B at 8.9 $\mu\text{m}$ .....	14
17.	Encircled energy and PSF cross section for long-wave CB-2B at 11.5 $\mu\text{m}$ .....	15
18.	Output fiber diagram for CB-2B.....	15
19.	Mixing rod operation for 3 inputs ( $F/2.5$ in air = $F/6$ in rod).....	16
20.	Ray trace and spot diagrams for CB-2B collimator.....	16

## TABLES

1.	CB-2 requirements .....	1
2.	Performance estimates for CB-2A .....	12
3.	Performance estimates for CB-2B .....	17



# **NEXT GENERATION LWIR SPECTRUM PROJECTOR (CB-2) DESIGN STUDY**

## **1. Introduction**

This document outlines the basic optical requirements for the next generation LWIR spectrum projector, the CB-2, and the two best ways to meet those requirements. Based upon the success of the CB-1 Spectrum Projector<sup>1</sup> built and tested by MRC, Dugway Proving Ground, Block Engineering and Edgewood Research Development and Engineering Center, a new and improved CB-2 is being designed. The preliminary designs for the CB-2 are enclosed along with their expected performances. Aspects for the CB-2 system not discussed in this paper are the drive electronics for the emitter array, the calibration procedure and requirements, and the necessary steps for making calibrated movies to drive the emitters.

## **2. CB-2 Requirements**

The requirements for the CB-2 set forth at a meeting with Dugway Proving Ground personnel in January 1999 are listed below.

**Table 1. CB-2 requirements.**

<b>Parameter</b>	<b>Required Value</b>
Total band	8 to 13.1 $\mu\text{m}$
Spectral Resolution – 8 to 10 $\mu\text{m}$	4 $\text{cm}^{-1}$
Spectral Resolution – 10 to 13 $\mu\text{m}$	16 $\text{cm}^{-1}$
Exit Pupil Diameter	3" or 76 mm (1" $\pm$ 1" for vibration)
UUT Field of View	1.5 x 1.5 degrees
Dynamic Frame Rate	30 Hz
Dynamic Radiance Modulation	5% for 300 K background
Blackbody and Dynamic Spectra	Spatially mixed to better than 10% (?) by area

## **3. CB-2 Design Overview**

The CB-2 will use one 512x512 NODDS infrared emitter array as the source for the dynamic spectrum and a blackbody for the static, but variable, background spectrum. The dynamic spectrum is produced by using the emitter array as the source in a grating spectrometer. The array can be driven at rates up to 60 Hz. An exit slit is used to limit the projected bandwidth from a given emitter display pixel (dixel). The grating groove density and the spectrometer focal length determine the total bandwidth dispersed across the emitter array. It is possible to either disperse all 5  $\mu\text{m}$  across a single stripe (several

columns and all rows) of the emitter array or segment the emitter array and disperse part of the 5  $\mu\text{m}$  across each section. The segmented approach adds complexity to the system but enables the resolution to be reduced.

The spectral resolution from an emitter dixel or group of dixels is controlled by the spatial resolution of the spectrum projector and the slit width. Since a typical FWHM spot diameter for a grating spectrometer is on the order of 50 to 100  $\mu\text{m}$ , the convolution of a typical emitter image and the exit slit is approximately equal to the sum of the spot diameter and the slit width. If 5  $\mu\text{m}$  is dispersed across the 1.0" emitter height, the slit width is 250  $\mu\text{m}$  and the spot diameter is 75  $\mu\text{m}$ , for instance, then the resolution will be  $5 \cdot (250 + 75) / 25400 = 64 \text{ nm}$ . In wavenumbers this corresponds to  $6.4 \text{ cm}^{-1}$  at 10  $\mu\text{m}$  and  $10 \text{ cm}^{-1}$  at 8  $\mu\text{m}$ .

To reduce the resolution to the levels listed in Table 1, our CB-2 design will use two sections. A stripe of emitters on one end of the emitter array will serve as the source for one section while a stripe of emitters on the opposite end of the array will serve as the source for the second section. Each half of the spectrum projector will have its own optics, grating and exit slit. The outputs from the two sections (following the exit slits) will be combined and added to light from the blackbody before being collimated. The output collimator will project an exit pupil (an image of the grating) onto the entrance aperture of the UUT spectrometer.

The radiance transfer from the emitter dixels to the UUT depends on a number of factors. The spectrum projector F/# determines the output collimator focal length (equal to 76 mm times the F/#) and the focal length times the UUT field of view determines the field size seen by the UUT at the exit slit plane. A narrower exit slit reduces the spectral resolution but it also reduces the relative signal received by the UUT. If the collimator focal length is 100 mm, for instance, the field seen by the UUT at the exit slit will be  $100 \cdot (1.5/57.3) = 2.62 \text{ mm square}$ . Since the dynamic spectrum only comes from the region occupied by the opening in the slit, the limiting radiance from the dynamic spectrum is proportional to the relative area of the field occupied by the slit. A 250  $\mu\text{m}$  wide-slit that is at least 2.62 mm high, for example, will occupy 9.5% of the field seen by the UUT. Since the emitters can be heated to a max. temperature of about 750 K, the maximum apparent temperature seen by the UUT will be about 185 K, assuming an emitter emissivity of 0.4, an emitter fill factor of .22 and a projector transmission of 0.3. This sounds quite low, but the normal emission or absorption from an airborne chemical agent only modulates the background radiance by about 2% of ambient. The apparent temperature of 2% modulation for a 300 K object is 165 K. The 185 K apparent temperature cited above corresponds to a radiance modulation of 5% at 300 K.

#### **4. CB-2 Design Trade-Offs**

There are at least two different ways to configure the CB-2, but in this document we will only present two. Both configurations use a dual grating spectramitter (spectra-emitter), some sort of dual exit slit and combiner, and an output collimator, but the type of grating spectramitter and slit design can vary greatly. The first CB-2 design is a refractive (lenses) one with plane transmission gratings, linear arrays of optical fibers as the exit slit, and a refractive collimator. The second CB-2 design is a reflective one with a convex reflection grating and a reflective collimator. The slit configuration for this spectramitter is a linear array of fibers followed by a mixing rod. These two separate designs are analyzed below and compared in section 5 to see how they meet the requirements in Table 1.

There are several features that both configurations share that can be discussed before analyzing their differences. One is that one emitter array will be used with one set of drive electronics. The two parts of the emitter array responsible for each spectral region can be controlled concurrently but independently. Spectral-varying movies will be made for the two halves of the dynamic spectra by applying voltages to the outer 96 or 144 columns (4.8 or 7.3 mm) of each half of the array. When the radiance for a given wavelength is to be changed all emitters along one edge of a given row will be driven to a new temperature. Another is that a new emitter dewar face plate must be made that allows the ZnSe vacuum window to be only half an inch from the emitter array. Another is that two fold mirrors with wedge-shaped edges along the edge closest to the emitters must be positioned just outside the dewar window to redirect the light from each half of the array towards the collimating optics and grating. The ray bundles from each emitter on the array are centered along the normal to the array, so the wedged-edges of the mirrors will be very close together along the plane through the middle of the emitter array. A fourth common feature is that a second fold mirror will be used to redirect the light approaching the exit slits towards a common location in order to either shorten the required fiber length. A fifth common feature is that either system will be at ambient laboratory temperature and atmospheric pressure, and the blackbody used will have a 2" or larger square thermo-electric heater source to facilitate quick adjustment of the background temperature. A sixth feature in common is that a 3" diameter exit pupil will be projected out about 4 to 9" in front of the last element to facilitate coupling to the UUT while it is on the vibration table. The details of the refractive system are presented next.

##### **4.1. Refractive Spectramitter, CB-2A**

The refractive spectrum projector system uses two identical lens trains consisting of a collimating quartet, a plane transmission grating, a re-imaging triplet, an exit slit consisting of a linear array of 16 optical fibers, and an output collimating quartet that projects the exit pupil 9" in front of the outer-most element. The lens elements are made from ZnSe and NaCl. The gratings are made from thallium bromoiodide (KRS-5). Two

fold mirrors are used in each half of the spectramitter and these are made from gold-coated pyrex or aluminum. The fibers are air-clad silver halide. They are 300  $\mu\text{m}$  in diameter and about 40 cm-long. The fibers from the two linear arrays are mixed together at the focus of the output collimating lens in a square array composed of 68 fibers. The other 36 fibers go to the blackbody. The fibers from the two spectramitter-halves and the blackbody are uniformly integrated in the output array.

The practice of designing a fast spectramitter system using lenses has its limitations. First of all, in the 12-13  $\mu\text{m}$  region there are not many user-friendly materials that transmit much light. Germanium works great up to about 11.5  $\mu\text{m}$ , but by 13  $\mu\text{m}$  its absorption exceeds 30% per cm. Other materials such as potassium bromide, cadmium telluride and potassium chloride are hygroscopic, toxic and/or too soft to work well. The two materials with the lowest absorption and best overall properties in the 7 to 13.5  $\mu\text{m}$  range are ZnSe and NaCl. The sodium chloride can be protected from moisture with an evaporated anti-reflection coating. A limitation on NaCl is that lenses must be smaller than 160 mm in diameter. Despite these limitations, we developed a design for an F/1.25 projector system. Both systems use plane transmission gratings made out of KRS-5. The KRS-5 is somewhat toxic, so gloves should be used when handling it, but gratings should not be handled much anyways.

#### 4.1.1. Fiber Exit Slit.

The exit slit is made up of a linear array of silver halide fibers. The advantage of using fibers is that the height of the fiber array can be made larger than the height of the field seen by the UUT, so the effective area at the collimator focal plane for each half of the spectramitter can be increased in this way. In this design the linear array is composed of 16 fibers while the square array at the collimator focus is a square with 9 columns of 8 and 7 fibers, nested together. The pattern is shown in Figure 1. The total number of fibers is 68 so the total size of the fiber array is about 2.5 mm (assuming half a mil spacing between fibers). Each half of the spectramitter contributes 23.5% of the fibers while the blackbody contributes 53%. The total area fill factor for each half of the dynamic spectrum is  $16(15^2\pi)/2.5^2 = 18\%$ . The area fill factor for the blackbody fibers is  $(36/16) \cdot 18 = 41\%$ . By contrast, the area of a normal slit, 300  $\mu\text{m}$ -wide by 2.5 mm high would be 12%. Therefore, as long as the transmission of the fibers is better than 67% the fibers should produce superior results. The spatial mixing of the different wavelengths at the output of the fiber array is about  $\frac{1}{2}$  of the field in each direction and 6.3% by area. If it is decided that this is not sufficient to uniformly fill the UUT detector then a mixing rod can be used immediately after the fibers (section 4.2.1).

The linear arrays have an effective slit width defined as follows. Although the diameter of the fiber cores is 300  $\mu\text{m}$ , the area occupied by the 16 fibers at their edge in the cross direction (perpendicular to the fiber stacking direction) is zero. Conversely the area in a

narrow strip along the diameters linking the fibers together is essentially equal to a rectangle of the same dimensions. Therefore, the area occupied by the fibers drops off as the cosine of the half-width normalized to  $\pi/2$ . The last 50  $\mu\text{m}$  of the radius of the fiber in the cross direction of the fiber array, for instance, only adds 16% to the total fiber area. A plot of the fiber area and the area of a normal rectangular slit as a function of the cross-direction half-width is shown in Figure 1. The width of the rectangle equals the total fiber area at a half-width of 115  $\mu\text{m}$ . For this reason we can estimate an effective slit width for the fibers to be 230  $\mu\text{m}$ . The idea of an effective width makes sense by considering that light from a single dixel projects a spectral continuum in the cross direction to the fiber array, but as the light at off-center wavelengths reach the fiber at larger half-widths they are attenuated by the reduction in fiber area. This tends to reduce the transmitted spectral bandwidth and improve the spectral resolution.

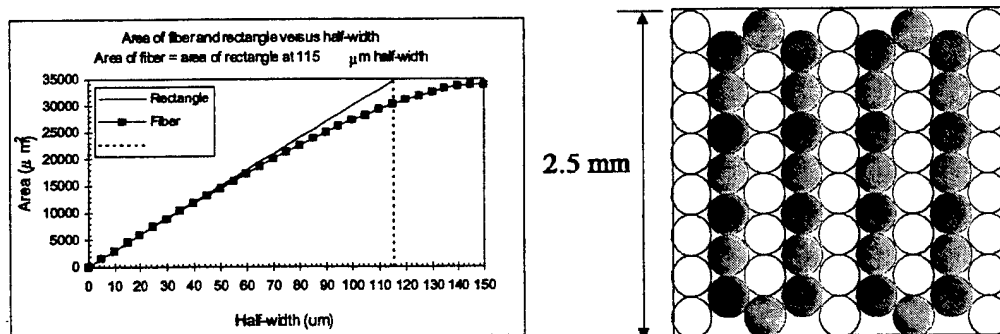


**Figure 1. (left) Fiber area variation with radius relative to ordinary slit. (right) View of output fiber array from perspective of UUT. Blue fibers are from the short-wave half, pink from the long wave half, and white are from the blackbody.**

The transmission of the silver halide fiber is very good in the 7 to 13  $\mu\text{m}$  range. A plot of the attenuation versus wavelength (from CeramOptec) is shown in Figure 2. Since we are expecting using fiber lengths on the order of 0.4 m or less, the expected transmission for all projected wavelengths should be twice as high as shown in Figure 3. In particular we expect the transmission for all wavelengths to exceed 90 %. There will be additional losses due to reflections off the ends of the fibers and from bends in the fibers, but we are planning to have anti-reflection coatings applied to the ends to reduce the reflection losses to less than 3% and the fibers will be configured with as few bends as possible to minimize those losses to less than 10%. The total transmission for the fibers should therefore easily exceed the 67% benchmark and probably be closer to 77% at all wavelengths in the 7 to 13  $\mu\text{m}$  range.

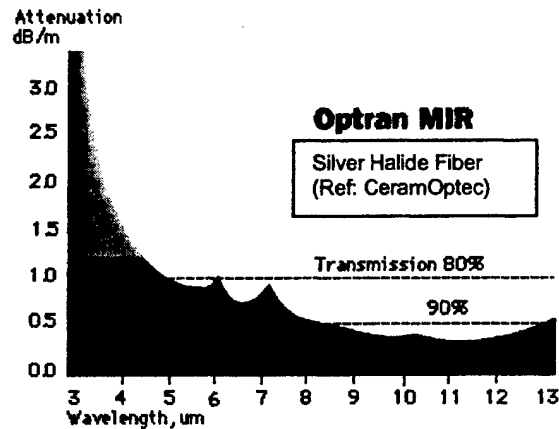


Figure 2. Silver Halide attenuation plot. For 30 cm lengths, the attenuation will be about a third of that in the graph. However, for air-clad fibers additional bend losses will offset that gain.

#### 4.1.2. CB-2A Optical Layout and Performance Estimates

The CB-2A is a refractive system with two halves. The layouts and performance estimates for the two halves are discussed separately.

##### 4.1.2.1. CB-2A Short Wave Analysis

Ray trace diagrams for the short-wave 8-10  $\mu\text{m}$  spectramitter are shown in Figures 3 and 4. The corresponding spot diagrams are shown in Figure 5, and encircled energy and PSF plots are shown in Figure 6. The RMS spot radius listed in the spot diagrams is

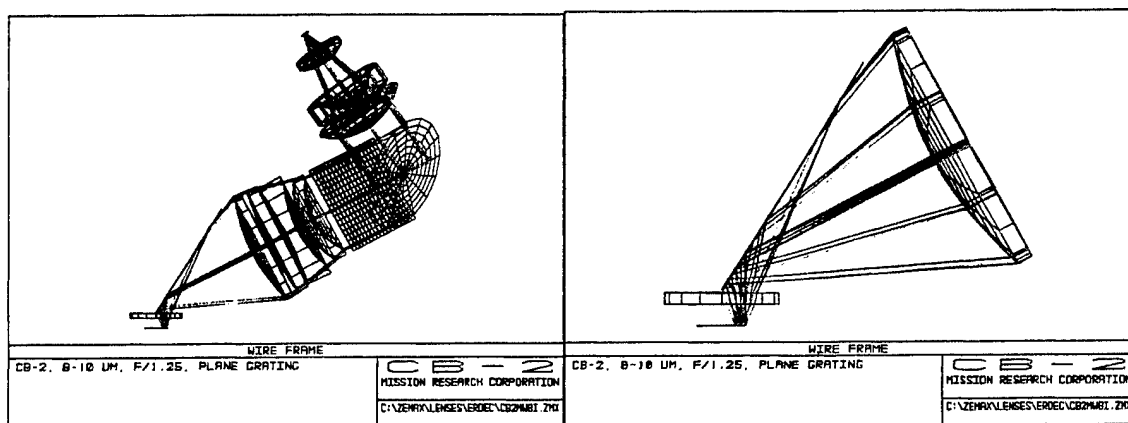


Figure 3. CB-2A short wave ray trace diagrams. (Left) Top view of emitter (colored by field). (Right) Close-up (colored by field)

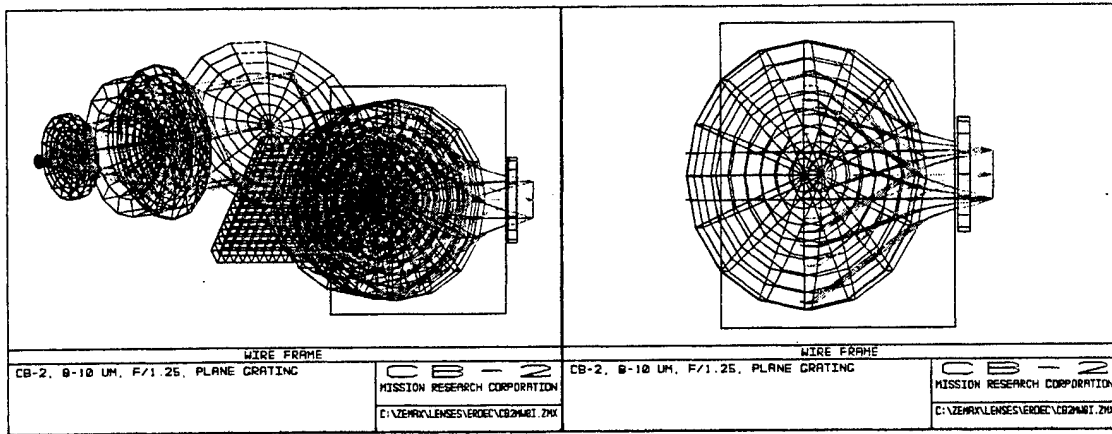


Figure 4. CB-2A short wave ray trace. (Left) Side view of emitter (colored by wavelength). (Right) Close up (colored by wavelength).

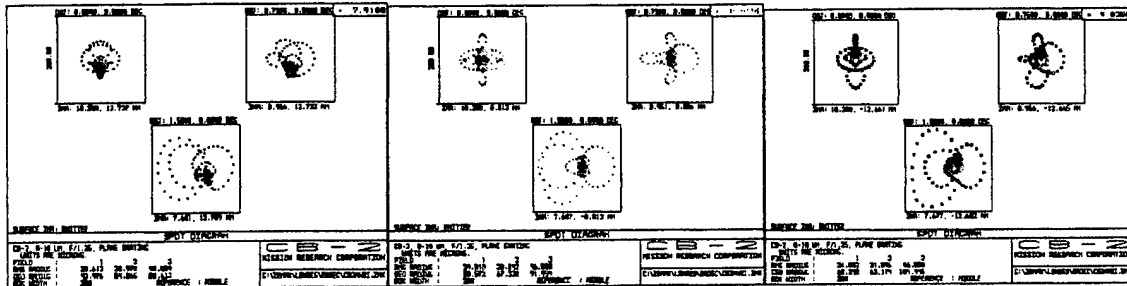


Figure 5. CB-2A short wave spot diagrams for three wavelengths.

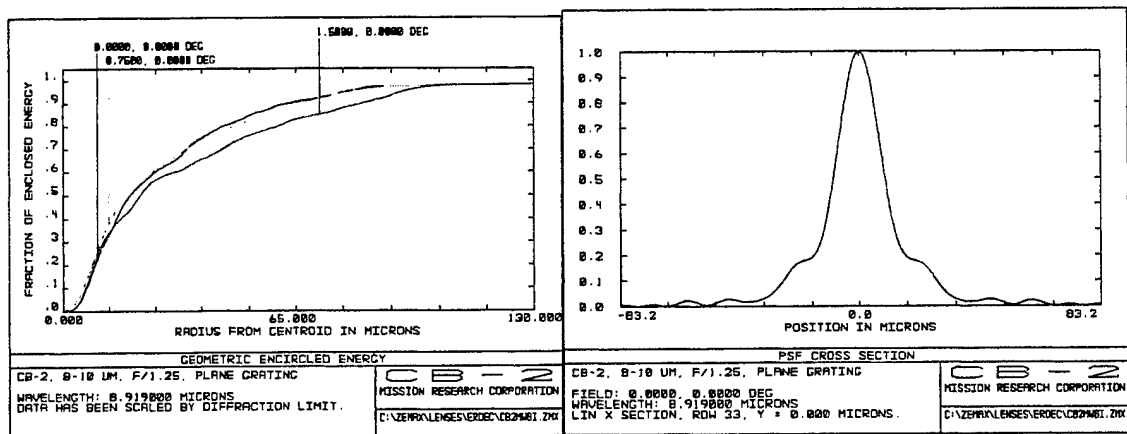


Figure 6. CB-2A short wave encircled energy and PSF plots for 9  $\mu$ m.

approximately the same as the half-width at half- maximum, so two times the RMS radius is equal to the full-width at half-maximum (FWHM). The FWHM spot size from a single emitter row will equal the convolution of the emitter width (about 25  $\mu\text{m}$ ) and the FWHM from the spot diagram (Figure 4). The spectral resolution from a single emitter row is computed from the convolution of the FWHM spot size, the dixel size and the exit slit width.

It is worth noting on the spot diagrams that for each wavelength the middle of the spots at the three field locations do not move around much in the y (wavelength-changing) direction. This means the “smile” of the spectramitter is low ( $< \pm 13 \mu\text{m}$  spatially or  $\pm 1 \text{ nm}$  spectrally), and that a particular emitter row will project light at only one wavelength (plus a nominal distribution) through the fiber slit. The encircled energy diagram shows that nearly all the light, at 11.565  $\mu\text{m}$ , in this case, is contained within a 110  $\mu\text{m}$ -radius for all field locations. The PSF cross section shows the same information in another format.

#### 4.1.2.2. CB-2A Long Wave Analysis

The Ray trace diagrams for the 10-13  $\mu\text{m}$  spectramitter are shown in Figures 7 and 8. The spot diagrams are shown in Figure 9, and the encircled energy and PSF plots for 11.6  $\mu\text{m}$  are shown in Figure 10.

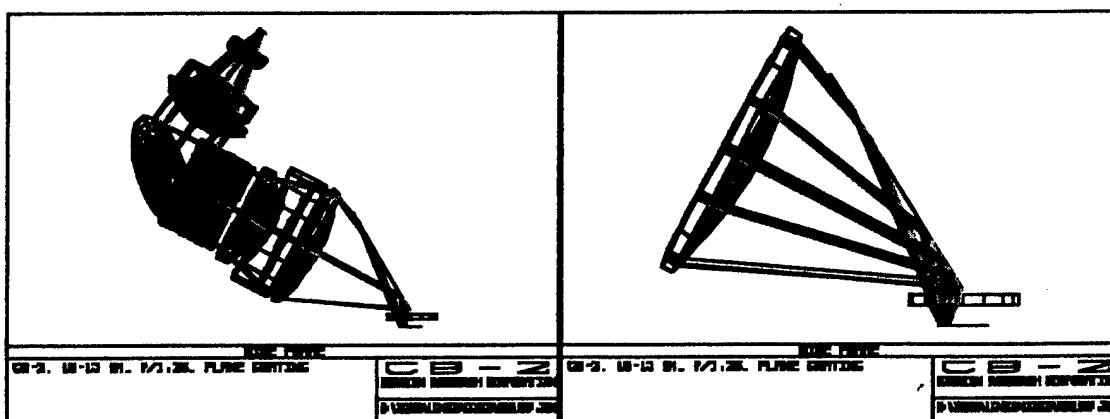


Figure 7. CB-2A long wave ray trace diagrams. (Left) Top view of emitter, colored by fields. (Right) Close-up, colored by fields.



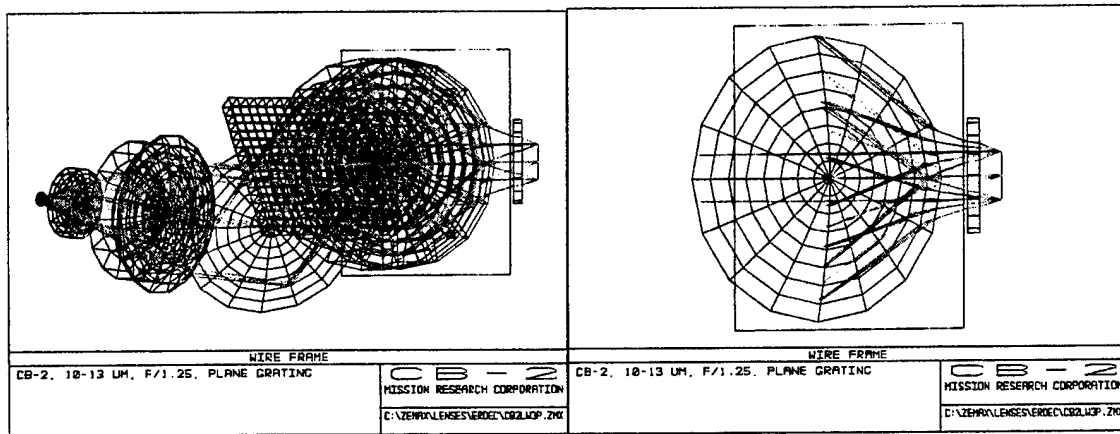


Figure 8. CB-2A long wave ray trace diagrams. (Left) Side view of emitter (colored by wavelengths). (Right) Close-up (colored by wavelengths).

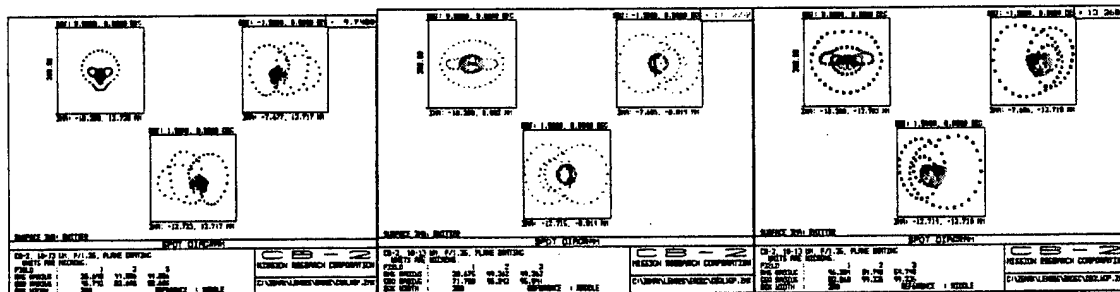


Figure 9. Spot diagrams for long-wave CB-2A. Notice the consistency of the 'y' image ordinate for each wavelength (variation  $< \pm 13 \mu\text{m}$ ). This indicates low distortion and "smile".

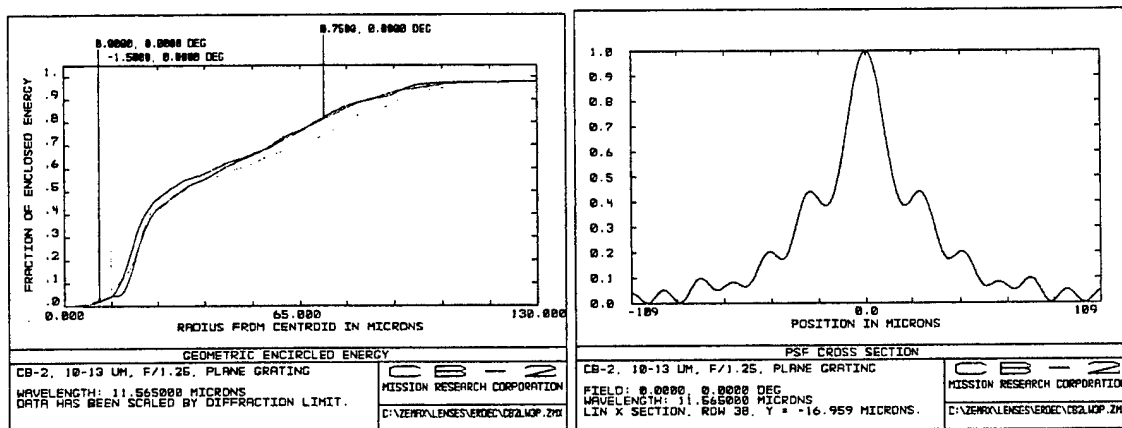


Figure 10. CB-2A Spot diagrams and encircled energy diagrams for 11.6 μm.

### 4.1.3. CB-2A Output collimator

The output collimator is an achromatic refractive lens system made from ZnSe and NaCl. It has two elements of each material. The two ZnSe elements have an aspheric surface. This lens projects a 3" diameter pupil 9" in front of the first element. This is approximately where the UUT entrance pupil should be located. Ray trace and spot diagrams, shown in Figure 11, indicate the lens is diffraction limited.

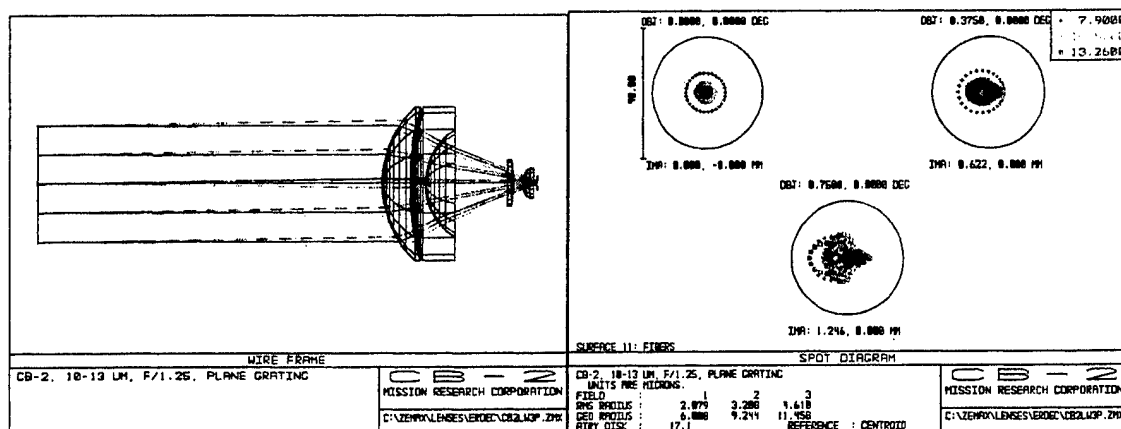


Figure 11. CB-2A collimator ray trace diagram and spot diagrams. The small spots indicate excellent performance.

### 4.1.4. CB-2A Conceptual Layout Diagrams

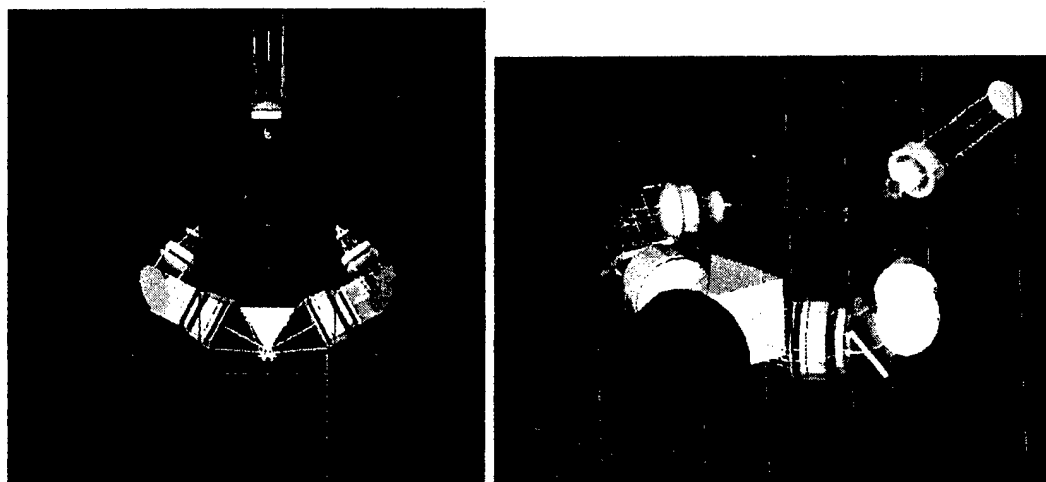
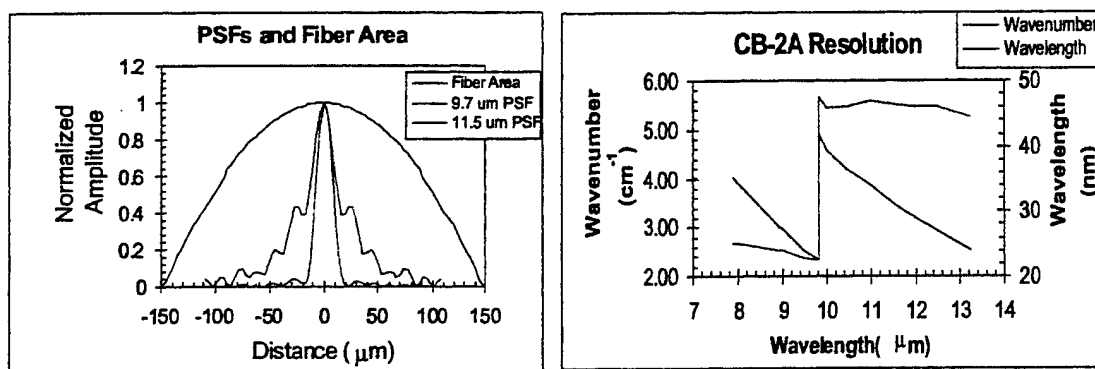


Figure 12. Top and perspective views of conceptual layouts of the CB-2A system. The middle fiber bundle goes to the blackbody (not shown) which can be mounted on a stand above the specramitters.

#### 4.1.5. CB-2A Spectral Resolution

The expected spectral resolution as a function of wavelength can be found several ways. One is to convolve the PSFs with the dixel width (25  $\mu\text{m}$ ) and the fiber area curves of Figure 13 and then multiply the result by the spectral dispersion factor, the number of nm per  $\mu\text{m}$  across the emitter array. Note that the PSF of the 9.7  $\mu\text{m}$ -spot in Figure 7 is about 20 to 25  $\mu\text{m}$  FWHM and this equals the RMS radius in the spot diagram in Figure 6. The second is to actually alter the wavelengths for a middle field location in Zemax and note the wavelength for which the center of the spot has moved plus or minus  $115+13+\text{spot radius } \mu\text{m}$ , the 13  $\mu\text{m}$  being added for the dixel half-width. The latter method was used to compute the spectral resolution for this spectramitter design, the results of which are shown in Figure 13.



**Figure 13. (Left) Fiber area profile and typical emitted PSF for CB-2A. (Right) CB-2A predicted spectral resolution. The discontinuity at 9.9  $\mu\text{m}$  is where the radiance source changes from the short wave to the long-wave spectramitter half.**

#### 4.1.6. CB-2A Radiance Estimates

The estimated radiance at each wavelength can be determined by starting with an emitter dixel at a peak kinetic temperature of 740 K and then scaling the radiance from this source by losses in the system. The loss mechanisms are: dixel fill factor, dixel emissivity, optics reflections, optics absorption, grating in-efficiency, fiber reflections, fiber absorption, fiber bend losses, and relative fill factor of fiber areas. These values are listed in the table below.

#### 4.1.7. CB-2A Performance Estimates

The following table lists the performance estimates for the CB-2A.

**Table 2. Performance estimates for CB-2A.**

Total Band	7.9 to 13.25 $\mu\text{m}$
Spectral Resolution, 8-10 $\mu\text{m}$	< 4 $\text{cm}^{-1}$
Spectral Resolution, 10-13 $\mu\text{m}$	< 6 $\text{cm}^{-1}$
Projector F/#	1.25
Exit Pupil Diameter	76 mm
Collimator Focal length	95 mm
UUT Field height	2.5 mm
Fiber areas: SW, LW and BB	1.13, 1.13 and 2.54 $\text{mm}^2$
Fill Factor for active area per dynamic wavelength	18%
Total Number of surfaces per band (less fibers)	28
Estimated avg. reflection per surface	0.9%
Total reflection loss at 9 or 11 $\mu\text{m}$	22.4%
Total thickness ZnSe, NaCl, KRS-5	113 mm, 37 mm, 12 mm
Total absorption loss at 9 or 11 $\mu\text{m}$ for each matl.	1%, 0.1%, 1%
Grating efficiency	55%
Fiber transfer efficiency for 30 cm length and AR	77%
Total transmission factor of optics	$.77 \cdot .55 \cdot .77 \cdot .18 = 5.9\%$
Spatial/spectral mixing percentage per area	5.8% (all wavelengths in each _ of side of field)
Modulation % for 300 K	7.2 % (assuming 196 dixels or 2 rows on per wave) 3.6% for one row of emitters per wave (at 9 $\mu\text{m}$ )
Spectral Radiance for single emitter row, at 9 $\mu\text{m}$	35 $\mu\text{W}/\text{cm}^2\text{-sr-}\mu\text{m}$
Spectral Radiance for all emitter rows, at 9 $\mu\text{m}$	136 $\mu\text{W}/\text{cm}^2\text{-sr-}\mu\text{m}$

#### 4.2. CB-2B Reflective Spectramitter

The CB-2B also uses one 512x512 NODDS emitter array and has two spectramitter halves. The spectramitter relays in this system are reflective. They consist of Offner relays with a grating as the secondary mirror. This type of system, for F/#s above 2.4, has very good performance in terms of distortion and aberrations. Each Offner will use a total of 144 columns (versus 96 for the CB-2A) and 512 rows of emitters to provide the dynamic signal. The NODDS array is placed at the object plane of two Offner spectrometers. Each Offner collects light from the 144 columns (rows vary with wavelength) at opposite ends of the NODDS array. The primary mirrors have radii of curvatures of 500 mm and the secondaries (gratings) have radii of 250 mm. The F/# of the CB-2B is 2.5. For F/#s below 2.5 the spot diameters increase above acceptable levels.

The short wave Offner will be designed to disperse light in the 7.90 to 9.945  $\mu\text{m}$  range. The grating will have 49 gr/mm. The dispersed light is focused into a linear array of 24 silver halide fibers. The fibers are identical to those used in the CB-2A except their length can be only 15 cm because the outputs of the Offner relays can be very close together. The height of the linear array of fibers will be about 7.6 mm (equaling the width of 144 emitter columns plus a fiber diameter). The transmission in the 7.9-9.95  $\mu\text{m}$  range for these fibers is about 85% (assuming the ends are AR coated).

The second, long wave, Offner will be designed to disperse light in the 9.8 to 13.25  $\mu\text{m}$  range. The grating will have 29 gr/mm. It is otherwise identical to the short wave Offner. The dispersed light is focused into another linear array of 24 silver halide fibers. The fiber configuration for this spectramitter half will be identical to the short wave half. The transmission in the 9.8 to 13.25  $\mu\text{m}$  range exceeds 85% (assuming the ends are AR coated).

The following ray trace shows a view of the NODDS array coupled to one of the Offners (7.9 to 9.95  $\mu\text{m}$ ). The Offner is tilted to the left to ensure the rays after the first fold mirror do not run into the emitter dewar (in line with the window shown). The rays do not actually run into the secondary mirror as they appear because the secondary is displaced out of the plane exit slit by 2". A spot diagram is shown for the middle wavelength of 8.92  $\mu\text{m}$ . The RMS spot radii for all fields are greater than that for the CB-2A while the geometrical radii are smaller. This means the FWHM is larger while the Airy disc is smaller. Figures 15 through 17 show the ray trace diagram, spot diagrams, encircled energy plots and PSF cross section plots for the short and long-wave halves of the CB-2B.

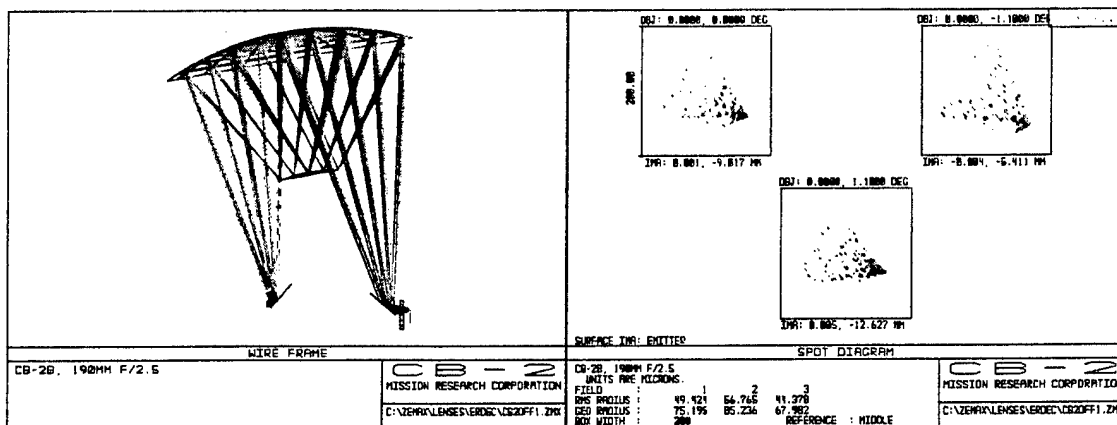


Figure 14. Ray trace diagram and spot diagram for short wave CB-2B.

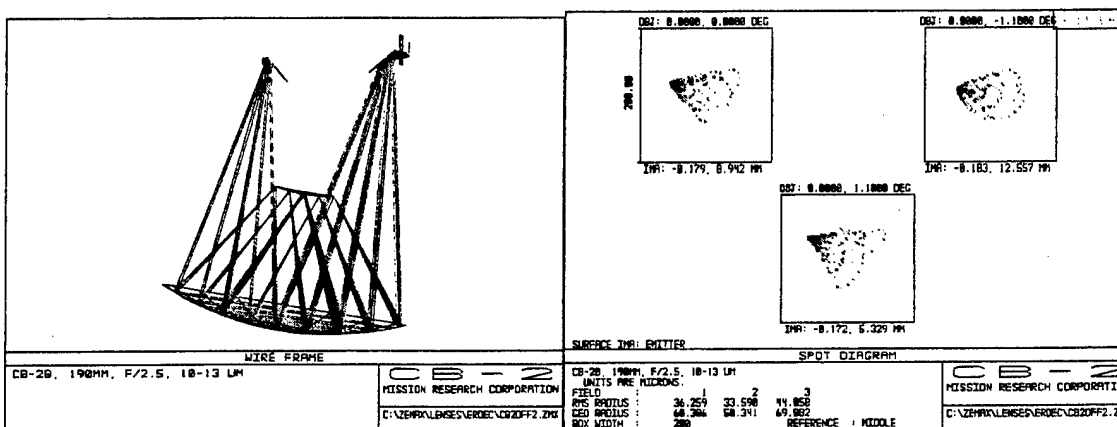


Figure 15. Ray trace and spot diagrams for long-wave CB-2B. Generally, the spot diameters are a little smaller than for the short-wave because the grating blaze angle is smaller.

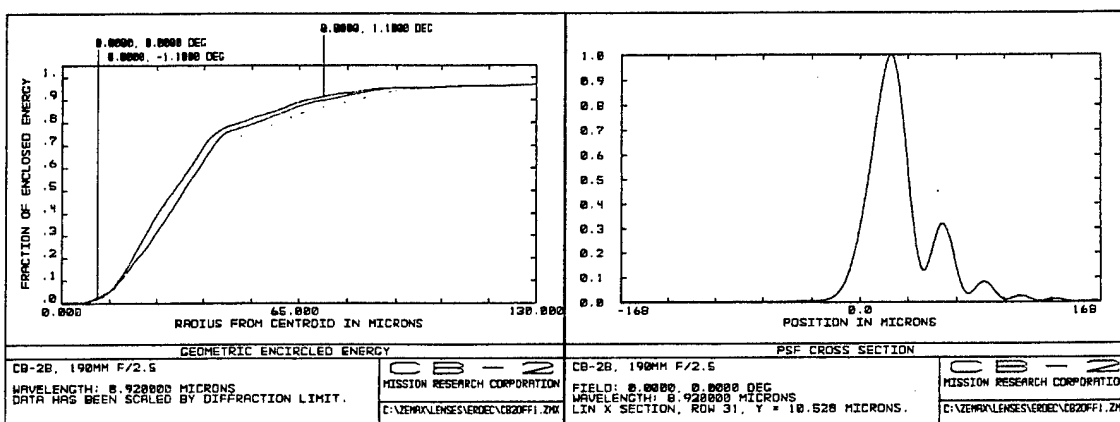


Figure 16. Encircled energy diagram and PSF cross section for short wave CB-2B at 8.9  $\mu\text{m}$ .

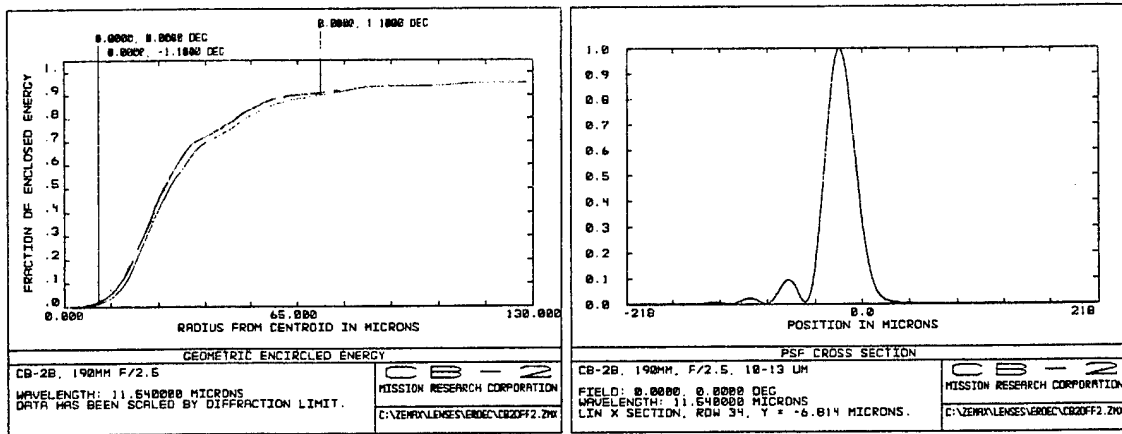


Figure 17. Encircled energy and PSF cross section for long-wave CB-2B at 11.5  $\mu\text{m}$ .

#### 4.2.1. CB-2B Output Fiber Array and Mixing Rod

To achieve a 76 mm diameter exit pupil, the focal length of the output collimator must be 190 mm for the F/2.5 Offiners. The 1.5 degree FOV from the UUT means the field seen by the UUT at the focus of the collimator will be 5.0 mm square. The output ends of the two linear fiber arrays will be grouped into a rectangular bundle, 5 mm by 1 mm, with the fibers from each band intermixed. The remainder of the field seen by the UUT will be filled by a small mirror at 45 degrees. This mirror will reflect light from a blackbody into the plane of the fiber outputs. Diagrams of the output fiber array are shown in Figure 18 below.

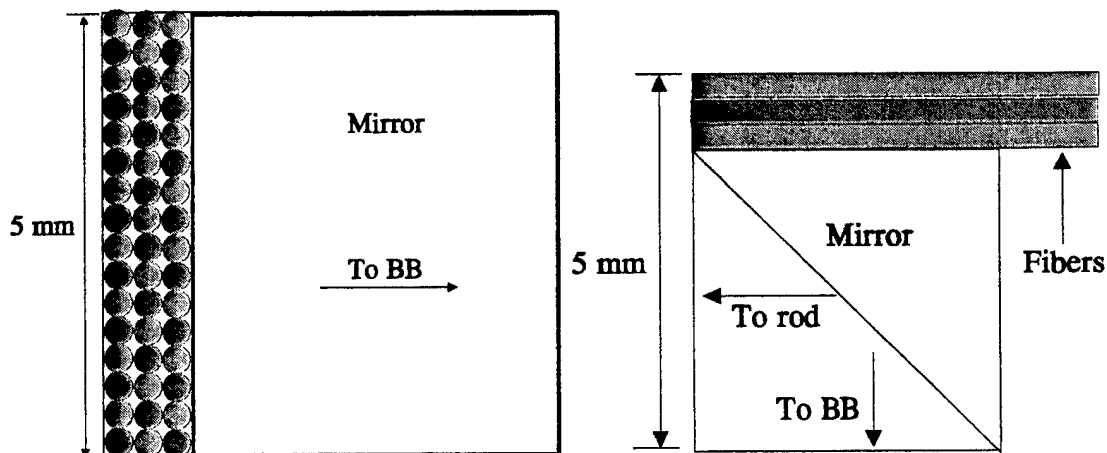
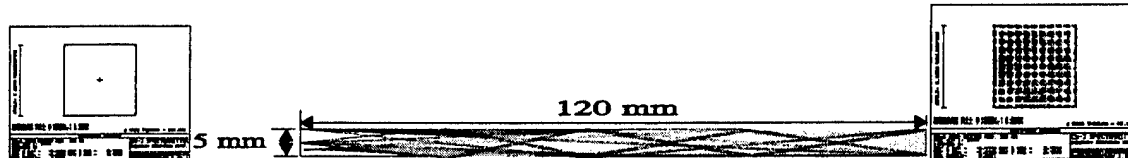


Figure 18. Output fiber diagram for CB-2B. The region on the right is occupied by a mirror that reflects the blackbody signal.

To spatially mix the light from the fibers and the blackbody a ZnSe light pipe will be used. The dimensions of the mixing rod will be 5 x 5 x 120 mm. The four long sides of

the rod will be uncoated while the ends will be AR coated for 7.9 to 13.3  $\mu\text{m}$  transmission. The index of ZnSe is 2.4 so the critical angle for total internal reflection is 65 degrees (relative to sides). Since the fibers emit light at only 12 degrees (and that is all that is needed from the BB), the ZnSe will reduce the angle by 2.4 to 4.8 degrees, so the light will easily be reflected along the sides. The absorption of this mixing rod will be about 1% and the reflection losses should be less than 3%, so the total transmission should exceed 96%. Figure 19 shows a cartoon of how light emitted from the fibers at the corners in the left image and various positions in the center diagram will be uniformly mixed at the end of the rod in the center diagram and the right image.



**Figure 19. Mixing rod operation for 3 inputs ( $F/2.5$  in air =  $F/6$  in rod). The light from all locations is uniformly mixed at the right end of the rod.**

#### 4.2.2. CB-2B Output Collimator

The collimator for the CB-2B is a refractive system similar to that for the CB-2A. The focal length for this lens, however, is 190 mm so the  $F/\#$  is 2.5. The number of lenses and the materials are the same as for the other collimator. A reflective off axis collimator could be used instead, however such a system occupies more space and does not have quite the performance of the lens system for ensuring the paraxial rays for each field location is normal to the mixing rod face. The ray trace and spot diagrams are shown in Figure 20. The spot diameters are nearly diffraction limited.

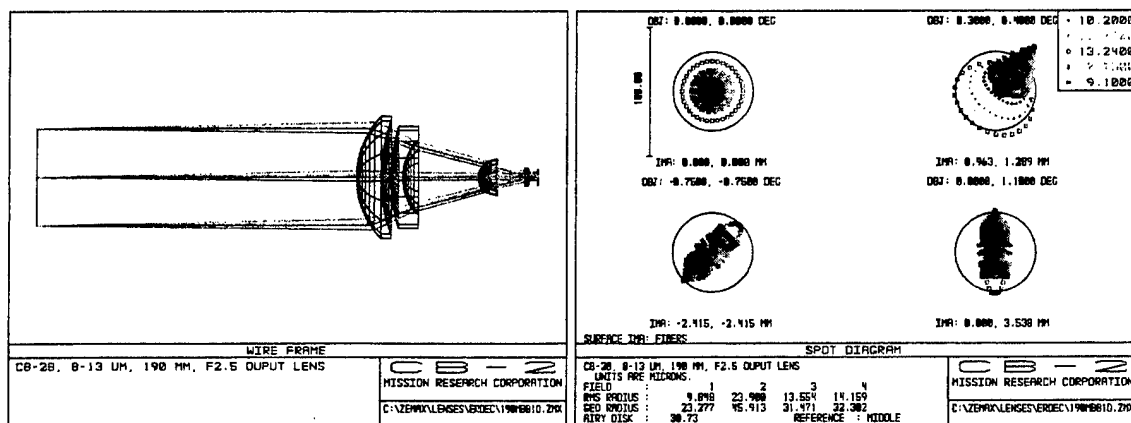


**Figure 20. Ray trace and spot diagrams for CB-2B collimator.**



### 4.2.3. CB-2B System Performance

The performance of the CB-2B is comparable to the performance of the CB-2A in the following areas: total band, band per spectramitter half, and spectral resolution. This is because the spot sizes from both systems are about the same and the same fibers are used as exit slits in both systems. The main difference, however, is in terms of the radiance output. The estimates for the CB-2B are listed in Table 3 below.

**Table 3. Performance estimates for CB-2B.**

Total Band	7.9 to 13.25 $\mu\text{m}$
Spectral Resolution, 8-10 $\mu\text{m}$	< 4 $\text{cm}^{-1}$
Spectral Resolution, 10-13 $\mu\text{m}$	< 6 $\text{cm}^{-1}$
Projector F/#	2.5
Exit Pupil Diameter	76 mm
Collimator Focal length	190 mm
UUT Field height	5.0 mm
Band areas: SW, LW (fibers) and BB (mirror)	1.69, 1.69 and 20.5 $\text{mm}^2$
Fill Factor for active area per dynamic wavelength	6.8%
Total Number of surfaces per band (less fibers)	8
Estimated avg. reflection per surface	0.9%
Total reflection loss at 9 or 11 $\mu\text{m}$	7%
Total thickness ZnSe	56 mm
Total absorption loss at 9 or 11 $\mu\text{m}$	1%
Grating efficiency	65%
Fiber transfer efficiency for 30 cm length and AR	85%
Total transmission factor of optics	$.92 \cdot .65 \cdot .85 \cdot .068 = 3.46\%$
Spatial/spectral mixing percentage per area	<0.25% (all wavelengths in 1/20 of side of field)
Modulation % for 300 K	4.2% (assuming 288 dixels or 2 rows on per wave) 2.1% for one row of emitters per wave (at 9 $\mu\text{m}$ )
Spectral Radiance for single emitter row, at 9 $\mu\text{m}$	21 $\mu\text{W}/\text{cm}^2\text{-sr-}\mu\text{m}$
Spectral Radiance for all emitter rows, at 9 $\mu\text{m}$	80 $\mu\text{W}/\text{cm}^2\text{-sr-}\mu\text{m}$

## 5. System Comparisons and Discussion

From Table 3 above and Table 2 previously, the main difference between the two systems is in the projected radiance. The CB-2B system can emit  $21 \mu\text{W}/\text{cm}^2\text{-sr-}\mu\text{m}$  from one emitter row, while the CB-2A can emit  $35 \mu\text{W}/\text{cm}^2\text{-sr-}\mu\text{m}$  at  $9 \mu\text{m}$ . Another difference is that the CB-2B requires more fibers per spectramitter half, but the total number of fibers is a little less and each fiber can be half the length as with the CB-2A. The total number of fibers in the CB-2B is 48 while that in the CB-2A is 68. The footprint of the CB-2B is slightly larger than the footprint of the CB-2A, but the difference is not significant. The complexity of the CB-2A system is greater than that of the CB-2B system, and it is likely that the cost of the CB-2A system will be higher than that of the CB-2B system.

The choice of which system to go with really depends on how important the spectrally dynamic radiance is for the tests to be performed on the JSLSCAD. If powers above  $21 \mu\text{W}/\text{cm}^2\text{-sr-}\mu\text{m}$  are required for a resolution of about  $3 \text{ cm}^{-1}$  at  $9 \mu\text{m}$ , then the CB-2A is the system to go with. If powers below  $21 \mu\text{W}/\text{cm}^2\text{-sr-}\mu\text{m}$  are acceptable then the CB-2B may be the simpler and cheaper system.

Either system, however, will enable the JSLSCAD program to enter into the realm of virtual testing. This mode of testing is now a mainstay of the FLIR and IR imaging characterizations that are done at many US test centers. In fact, RTTC is about to receive a top of the line LWIR scene generator for testing IBAS and ITAS imaging sensors in a hardware in the loop fashion. This type of testing has been shown to enable the sensors to be characterized more accurately than other types of testing, including field tests, because all variables can be controlled. This same type of accomplishment could be achieved on testing of the JSLSCAD with the use of the CB-2 LWIR spectrum projector. MRC has plans for similar spectrum projectors in other bands such as the MWIR, visible and UV. Spectrum projectors covering all these bands would satisfy the requirements for HWIL testing of all nearly all standoff spectrometers.

### Reference

Thomas, M.C. , T.E. Old, R.W. Hendrick; "Performance characteristics of the CB-1 LWIR variable spectrum projector"; *Scientific Conference on Chemical and Biological Research, ERDEC '98, Session 1: Modeling and Simulation, Nov. 17, 1998.*